Rem: Revista Escola de Minas
ISSN: 0370-4467
editor@rem.com.br
Escola de Minas
Brasil

Ramos Ribeiro, Tiago; Leite de Lima, Moysés; Aquino Martorano, Marcelo; Batista Ferreira Neto, João
Silicon refining by a metallurgical processing route
Rem: Revista Escola de Minas, vol. 66, núm. 4, octubre-diciembre, 2013, pp. 479-484
Escola de Minas
Ouro Preto, Brasil

Metalurgia e materiais
Metallurgy and materials

Silicon refining by a metallurgical processing route

Rota metalúrgica para refino de silício

Tiago Ramos Ribeiro
Assistant researcher at the Institute for Technological Research of the São Paulo state – IPT and graduate student at Department of Metallurgical and Materials Engineering, University of São Paulo.
tiagorr@ipt.br

Moysés Leite de Lima
Assistant researcher at the Institute for Technological Research of the São Paulo state – IPT and graduate student at Department of Metallurgical and Materials Engineering, University of São Paulo.
mllima@ipt.br

Marcelo Aquino Martorano
PhD, Professor at the Department of Metallurgical and Materials Engineering, University of São Paulo.
martoran@usp.br

João Batista Ferreira Neto
PhD, Researcher at the Institute for Technological Research of the São Paulo state – IPT.
jbfn@ipt.br

Resumo

Experimentos de solidificação direcional foram realizados em um forno do tipo Bridgman para remoção de carbono e impurezas metálicas contidas no silício. Para remoção de carbono, a solidificação se deu pela extração do molde da zona quente para a zona fria do forno, enquanto que, para remoção de impurezas metálicas, a solidificação foi conduzida pelo resfriamento do forno sem a movimentação do molde. Nos experimentos para remoção de carbono, uma velocidade de extração do molde de 5 μm/s resultou em lingote com macroestrutura colunar de grãos alinhados ao seu eixo central e macrossegregação de carbono e partículas de SiC para o topo do lingote. No entanto, na velocidade de 80 μm/s, a macroestrutura consistiu de grãos colunares e alinhados na direção radial com partículas de SiC encontradas em todo o lingote, mesmo havendo maiores concentrações de carbono no topo do lingote, o que mostra uma macrossegregação menos severa. No experimento de remoção de impurezas metálicas, uma macroestrutura de grãos colunares alinhados ao eixo central do lingote foi obtida e os perfis de concentração de impurezas mostraram que houve macrossegregação para o topo do lingote.

Palavras-chave: Refino de silício, solidificação direcional, remoção de carbono, macrossegregação.

Abstract

Directional solidification experiments were carried out in a Bridgman furnace to remove carbon and metallic impurities from silicon. For carbon removal, solidification was achieved by extracting the mold from the hot into the cold zone of the furnace, while for the removal of metallic impurities, solidification occurred by cooling the furnace with a motionless mold. In the experiments of carbon removal, a mold extraction rate of 5 μm/s results in an ingot with columnar grain structure aligned in the ingot axial direction and a macrosegregation of carbon and SiC particles to the ingot top regions. However, at a mold extraction rate of 80 μm/s, the grain structure consisted of columnar grains aligned in the radial direction and SiC particles were observed throughout the ingot, showing lower macrosegregation with a carbon concentration still larger at the ingot top. In the metallic impurities removal experiment, an ingot with a columnar grain structure aligned in the ingot axial direction was obtained and the concentration profiles showed significant metallic impurities macrosegregation to the ingot top.

Keywords: *Silicon refining, directional solidification, macrosegregation.*

1. Introduction

In the past decades, there has been increasing interest in energy generation, especially due to the environmental consequences of using nonrenewable sources, such as oil and mineral coal. The photovoltaic energy appeared as an alternative energy source, causing an increase in the installed worldwide capacity of almost 50 times from 2000 to 2011 (EPIA - European Photovotaic Indutry Association, 2012). Among the different materials used for the production of photovoltaic cells, silicon accounts for ~85% (Photon International, 2006). There are different silicon grades: metallurgical grade silicon (MGSi), solar grade silicon (SoGSi), and electronic grade silicon (EGSi). MGSi is the least pure (maximum impurity content of ~1 wt%) and is used in the aluminum and steelmaking industry. EGSi is the purest grade (maximum impurity content of ~1 ppbw) and is used in computer chips and other electronic devices. SoGSi is also very pure (maxium impurity content of ~1ppmw) and is used for solar applications.

At the beginning of the 90's, the demand for SoGSi was met by the scrap from the electronic industry. As this demand grew, an increase in SoGSi production at low costs was required, giving rise to new companies and processes specially focused on the solar market. Possible alternatives for SoGSi production are the processes based on recently-developed metallurgical operations. Intense research on the development of a metallurgical process route to produce SoGSi has been carried out in the Institute for Technological Research of São Paulo State (IPT). Different metallurgical operations, such as, plasma treatment, directional solidification, filtering, vacuum treatment, and slag refining are under investigation for removing impurities from MGSi. The main impurities that should be removed are metallic (Fe, Al, Ti, etc.), P, B, and C.

Carbon is present in Si as a dissolved element and as silicon carbide (SiC) particles. SiC hast wo deleterious effects for photovoltaic applications: it can cause wire breakage during silicon wafering and it can cause shunting in solar cells (Soiland, 2004). To remove carbon from silicon, Çiftja (Ciftja, 2009) studied silicon filtering using two types of foam filters: one made of SiC and another made of carbon. The author observed that SiC particles were well retained by SiC filters. The C filters reacted with silicon forming SiC particles and yielded a lower efficiency. Soiland (Soiland, 2004) studied the SiC formation and macrosegregation during silicon directional solidification, noting that SiC particles were pushed by the solidification front to the ingot top, which is the last region to solidify. Mühlbauer (Mühlbauer et al., 1991) conducted directional solidification of silicon in a Bridgman furnace to remove carbon and reported that, depending on the extraction velocity and crucible geometry, convection streams in the liquid caused SiC particles to remain in the liquid during solidification and, therefore, segregate to the ingot top. When interacting with an advancing solidification front, a particle can be pushed or engulfed. There is a critical front velocity for pushing/engulfment transition (PET). At velocities higher than the critical, particles are engulfed, while at lower velocities, particles are pushed ahead, remaining in the liquid. The critical velocity (v_{cr}) is given by (Stefanescu, et al., 1988):

$$v_{cr} = M \cdot R_p^{\,m} \quad m<0 \tag{1}$$

where R_p is particle radius and M and m are constants. Therefore, lower solidification front velocities are more likely to push and transport particles, such as SiC, to the ingot top, eliminating part of the carbon content and refining the original Si.

Metallic elements play an important role in the silicon used for photovoltaic purposes. As showed by Pizzini (Pizzini, 2012), the accepted concentration of metallic impurities depends on the macroscopic structure of the wafer (multi or single crystal), but it is always very low, because these impurities decrease photovoltaic cell efficiency. The directional solidification (DS) is an essential step of metallurgical routes to eliminate these metallic impurities and to produce SoGSi (Safarian et al., 2012). In the DS process, impurities are segregated to the last region to solidify, refining the remaining ingot.

Analytical models were proposed to investigate solute segregation during solidification considering a planar solid-liquid interface. Tiller et al. (Tiller et al., 1953) assumed solute transport only by diffusion (no convection). On the other hand, Scheil (Scheil, 1942) assumed a homogeneous solute distribution in the liquid, possibly under the effect of vigorous convection. Burton (Burton et al., 1953) studied an intermediate case in which convection is not vigorous enough to completely homogenize the liquid, but significantly affects solute transport. The authors (Burton et al., 1953) assumed a stagnant diffusion layer in the liquid adjacent to the planar solid-liquid interface and a homogeneous liquid out of this layer. In all these models the solute segregation during solidification strongly depends on the difference between the solute solubility in the liquid (C_L) and that in the solid (C_S) in thermodynamic equilibrium, characterized by the equilibrium partition coefficient (k_0) given below

$$k_0 = \frac{C_S}{C_L} \tag{2}$$

Segregation is more severe for lower partition coefficients, considering that $k_0<1$. Since most metallic elements have very small partition coefficients in silicon, they can be largely removed by solidification. Boron and phosphorus, however, have $k_0 \approx 1$, requiring other types of refining steps to be removed. Table 1 shows the partition coefficient of some impurities in silicon.

Kuroda and Saitoh (Kuroda & Saitoh, 1979) studied the macrosegregation of impurities in metallurgical silicon during solidification by the Czochralski method at velocities from 3 to 33 μm/s. They observed a decrease in macrosegregation when the solid-liquid interface apparently changed from planar to cellular. Yuge (Yuge et al., 2004) studied the macrosegregation of impurities during the solidification of metallurgical silicon in an electron beam furnace and observed a similar decrease in macrosegregation when the solid-liquid interface changed

from planar to cellular. Yuge (Yuge et al., 2004) also identified different macrostructure regions, namely, columnar, columnar/quasi-columnar, quasi-columnar, and dendritic, from the bottom to the top of the ingots.

The aim of the present work is to study the removal of metallic impurities and carbon from silicon by macrosegregation of these elements using directional solidification processes.

Element	K_0
Fe	8×10^{-6}
Al	2×10^{-3}
Ti	3.6×10^{-6}
V	4×10^{-6}
Mn	10^{-5}
B	0.716 - 0.8
P	0.35

Table 1
Equilibrium partition coefficient (k_0) of impurities in silicon (Martorano et al., 2010).

2. Experimental methods

Two different types of experiments were carried out in the present work to study the removal caused by macrosegregation of carbon and metallic impurities. In the first type, used for carbon removal, EGSi was first melted in a graphite crucible heated in a plasma furnace to be contaminated with carbon at the concentration of 0.12 ± 0.03 wt%. This carbon-contaminated EGSi was then re-melted in a Bridgman furnace (Figure 1A) inside a 30mm-diameter quartz mold coated with silicon nitride (Figure 1B). The furnace was heated to 1500°C and the furnace chamber was first evacuated to a 10 Pa inner pressure and then flushed with argon to the pressure of 0.07MPa. The mold was held in the furnace during 20 minutes for temperature stabilization and then was extracted from the furnace hot-zone at two different velocities: 5μm/s (experiment S30-5) and 80μm/s (experiment S30-80). After solidification and cooling to room temperature, the cylindrical ingots, with 30mm-diameter and 100mm height, were cut in their longitudinal section for macro and microstructure examination. Samples were also extracted from different positions along the ingot axis for chemical analysis.

In the second type of experiment, used to study the removal of metallic impurities, MGSi of about 99% purity (Fe = 1363 ppmw, Al = 445 ppmw, Ti = 117 ppmw, Mn = 216 ppmw) was used in a directional solidification experiment. The directional solidification furnace adopted for carbon removal was also adopted for removal of metallic impurities, but a graphite mold placed on the water cooled base was used, rather than a quartz mold. In this experiment, carbon contamination is not important. After melting and homogenization at 1550°C, the furnace was cooled at a controlled rate of 0.5°C/min down to 1000°C and turned off, without extracting the mold, as opposed to the experiment with carbon. The obtained ingot was cut in its longitudinal section for macro and microstructure examination. Samples were also extracted from different positions along the ingot axis for chemical analysis.

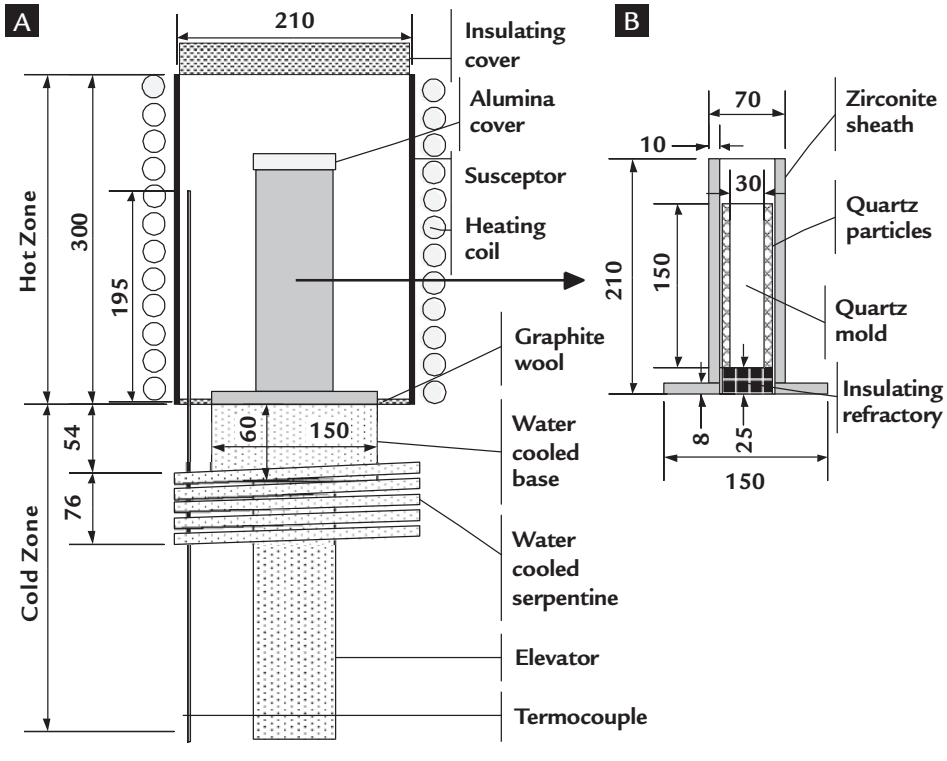

Figure 1
Bridgman type furnace used in the directional solidification experiments for carbon removal.
(A) Furnace scheme.
(B) Metal-container system (mold).
Sizes are in mm.

3. Results and discussion

Macrosegregation of carbon

Figure 2 gives the chemical analysis results showing increasing carbon content from ingot bottom to top for both experiments, with different extraction velocities. The concentration at the top of the ingot obtained from the S30-5 experiment is one order of magnitude higher than that in the S30-80 experiment, displaying a more intense macrosegregation of carbon.

Figure 3 shows the macrographs and micrographs at different distances from the ingot base obtained in these two experiments. The ingot from experiment S30-5 has a macrostructure of grains elongated and aligned in the axial direction. Some grains nucleated at the lateral wall, and grew to the ingot center, eventually bending upwards, especially in the lower parts of the ingot. Particles of SiC were only found at the ingot top, as shown in the micrographs (Figure 3A), being consistent with a larger carbon concentration at the top in the profiles of Figure 2. The ingot from experiment S30-80 has a macrostructure of columnar grains aligned in the radial direction. In this case, there were SiC particles spread throughout the ingot. At the ingot bottom, however, particles were smaller and in less number than those in other regions.

In these two experiments heat extraction occurs mainly through the mold lateral walls. When the mold is extracted from the furnace hot-zone at a sufficiently large velocity, the mold lateral wall is completely exposed to the cold-zone of the furnace, resulting in a radial heat extraction flux that causes the formation of columnar grains in the radial direction, as seen in the S30-80 ingot macrostructure (Figure 3B). On the other hand, for lower extraction velocities, the lateral wall of the mold lower part (containing solid) is exposed to the cold zone before the upper part (containing liquid) and remains in this position for a relatively long time due to the low velocity. Therefore, a significant amount of heat is transferred from the upper liquid to the cold region of the furnace using the underlying solid as a conduction path, rather than being transferred directly through the lateral walls. In this case, the heat flux is mainly axial in the middle and upper parts of the ingot, explaining the columnar grains aligned in the vertical direction observed in the S30-5 macrostructure (Figure 3A).

According to the calculations shown by Soiland (Soiland, 2004) for the critical velocity for PET in the SiC/Si system, particles with diameters up to 200 µm could be pushed up by a solid-liquid interface advancing at velocity of 80µm/s, which is the fastest velocity in the present work. All the particles observed in the micrographs were smaller than this size. For 5µm/s, the maximum particle diameter for pushing is 2000 µm, which is bigger than those that were observed. Therefore, in the two experiments, the solid-liquid interface velocity is low enough to push all SiC particles to the ingot top. Nevertheless, an accumulation of these particles at the top was only observed in the S30-5 experiment, while in the S30-80 experiments particles were spread all over the ingot. In the S30-5 experiment, owing to the lower solidification velocity, the solid-liquid interface was probably planar and moved upwards. Hence, it pushed the particles that were observed at the ingot top. For the larger solidification velocity (S30-80), however, the solidification front is more likely to be cellular or dendritic, which would entrap the particles in a net of ramifications, rather than push them to any part of the ingot. Therefore, particles would be spread throughout the ingot, as observed in the microstructures.

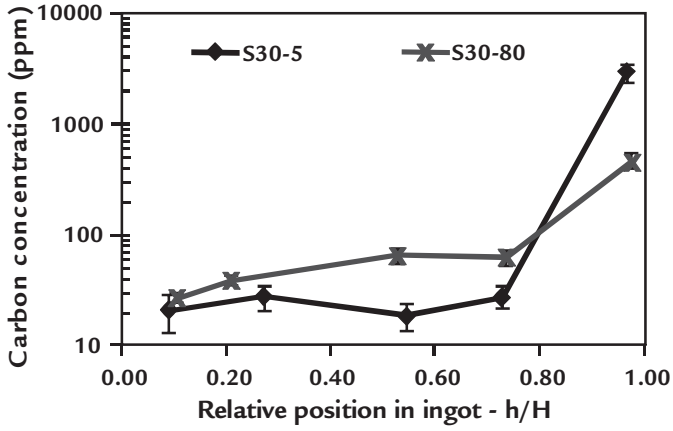

Figure 2
Carbon concentration as a function of the relative distance (h/H) along the ingots for S30-5 (5 µm/s) and S30-80 (80 µm/s) experiments, where h is the distance from the ingot base and H is the ingot length.

Macrosegregation of metallic impurities

The macro and typical microstructures of the longitudinal section of the ingot obtained in the study of metallic impurity removal are shown in Figure 4. From the ingot base up to 70 mm, there are columnar grains aligned in the vertical direction, which is a typical macrostructure of unidirectional solidification. At 70 mm, these columnar grains lost their common alignment, but still remained elongated. This grain macrostructure is similar to that observed by Yuge (Yuge et al., 2004). Intermetallic particles were found only in the upper part of the ingot, where grains were not completely aligned. The lower part of the ingot, however, was free from these particles (Figure 4), suggesting a macrosegregation of impurities from the ingot bottom to the top. Similar results were obtained by Martorano (Martorano et al., 2010). The transition region, at which intermetallic compounds were first seen, occurred at 75 mm from the ingot bottom.

The relative concentration profile for the main metallic impurities measured by ICP-OES is shown in Figure 5, indicating a macrosegregation of Fe, Mn, Ti, and Al to the ingot top, in

agreement with the microstructures. The concentrations of metallic impurities are lower than that in the metallurgical silicon (raw material) along 70 mm from the ingot base, in which no intermetallic compound was observed. These observations are similar to those described by Yuge (Yuge et al., 2004) and Kuroda (Kuroda & Saitoh, 1979).

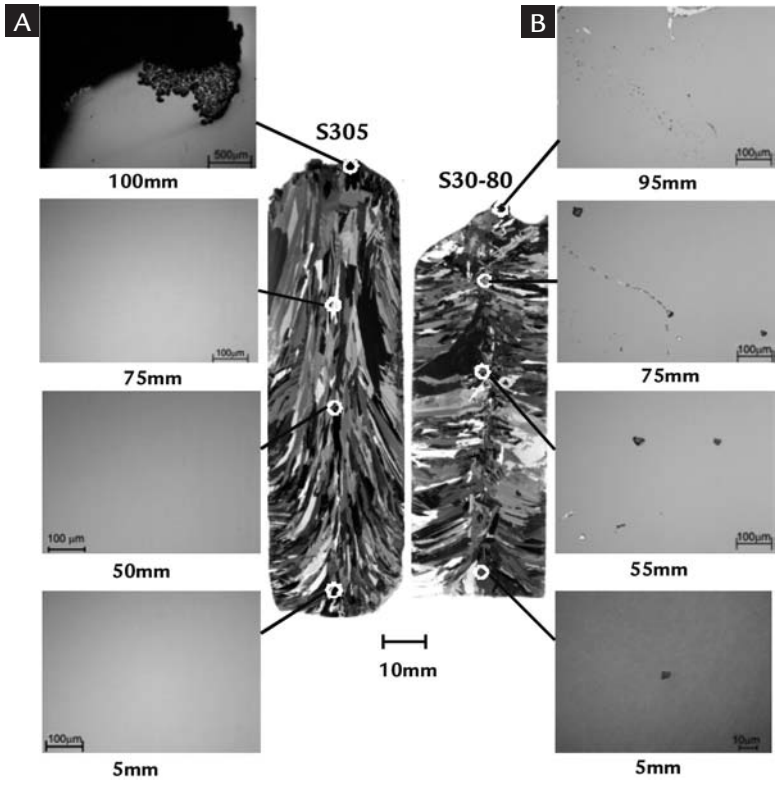

Figure 3
Macrographs and micrographs at different distances from the ingot base for experiments:
(A) S30-5 and (B) S30-80.

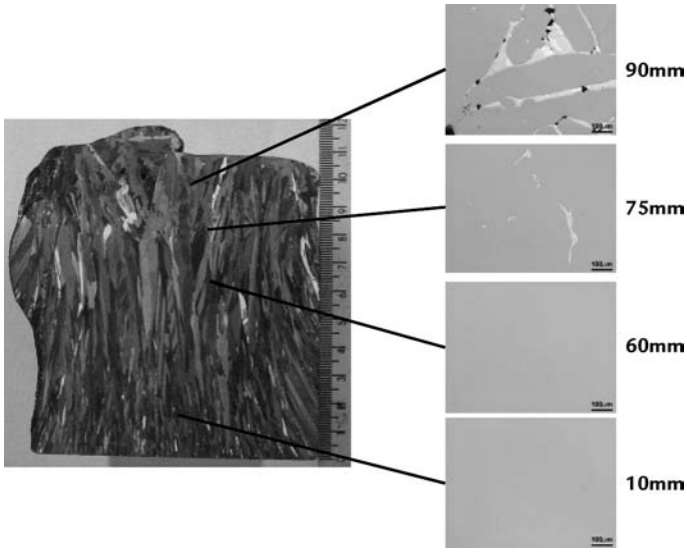

Figure 4
Macrostructure of the ingot longitudinal section and typical microstructures at different distances (indicated on the right) from the ingot bottom.

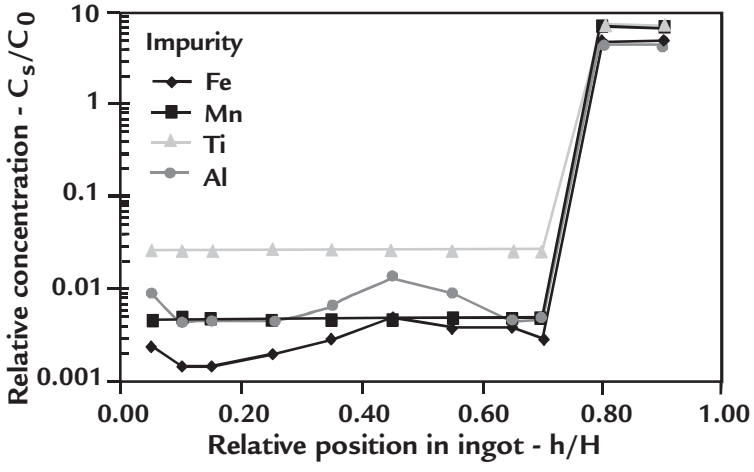

Figure 5
Relative concentration of Fe, Mn, Ti, and Al obtained by by ICP-OES as a function of the relative distance from the ingot base, where C_s and C_0 are the local and initial impurity concentration, respectively, h is the distance from the ingot base and H is the ingot length.

4. Conclusions

In the carbon removal experiments, a mold extraction rate of 5 µm/s results in an ingot with a columnar grain structure aligned in the ingot axial direction and a macrosegregation of carbon and SiC particles to the ingot top. However, at a mold extraction rate of 80 µm/s, the grain structure consisted of columnar grains aligned in the radial direction and SiC particles were observed throughout the ingot, although some macrosegregation is still observed as a result of a larger carbon concentration at the ingot top. In the experiment of metallic impurity removal, an ingot with a columnar grain structure was obtained again, with a macrosegregation of metallic impurities to the ingot top.

5. Acknowledgments

The authors thank the financial support from National Bank for Social and Economic Development (BNDES) and Cia. Ferroligas Minas Gerais (Minas-Ligas).

6. References

BURTON, J. A., PRIM, R. C., SLICHTER, W. P. The distribution of solute in crystals grown from melt. Part I. Theoretical. ***The Journal of Chemical Physics***, v. 21, p. 1987-1991, novembro, 1953.

CIFTJA, A. ***Solar silicon refining: inclusions, settling, filtration, wetting***. Trondheim: s.n., 2009.

EPIA - European Photovotaic Indutry Association, 2012. Global Market Outlook for Photovoltaics until 2016, Bruxelas, Bélgica.: s.n.

FLEMINGS, M. C. ***Solidification Processing***. s.l.: McGraw-Hill. 1974.

KURODA, E., SAITOH, T. Growth and characterization of polycrystalline silicon ingots from metallurgical grade source material. ***Journal of Crystal Growth***, v. 47, p. 251-260, 1979.

MARTORANO, M. A., FERREIRA NETO, J. B., OLIVEIRA, T. S., TSUBAKI, T. O., Macrosegregation of impurities in directionally solidified silicon. ***Metallurgical and Materials Transactions A***., 2010.

MÜHLBAUER, A., DIERS, V., WALTHER, A., GRABMAIER, J. Removal of C/SiC from liquid silicon by directional solidification. ***Journal of Crystal Growth***, v. 1, n.108, p. 41-52, 1991.

PHOTON INTERNATIONAL, 2006. Issue March.

PIZZINI, S. Towards solar grade silicon: challenges and benefits for low cost photovoltaics. ***Solar Energy Materials & Solar Cells***, p. 1528-1533, 2012.

SAFARIAN, J., TRANELL, G., TANGSTAD, M. Process for upgrading metallurgical grade silicon to solar grade silicon. ***Energy Procedia***, v. 20, p. 88-97, 2012.

SCHEIL, E. Bemerkungen zur schichtkristallbildung. ***Zeitschrift für Metallkunde***, p.70-72, 1942.

SOILAND, A.-K. ***Silicon for Solar Cells***, Trondheim: s.n., 2004.

STEFANESCU et al. Behavior of ceramic particles at the solid-liquid metal interface in metal matriz composites. ***Metallurgical Transactions A***, v. 19, n. 11, p. 2847-2855, 1988.

TILLER, W. A., JACKSON, K. A., RUTTER, J. W., CHALMERS. The redistribution of solute atoms during the solidification of metals. ***Acta Metallurgica***, p. 428-437, 1953.

YUGE, N., HANAZAWA, K., KATO, Y. Removal of metal impurities in molten solicon by directional solidification with electron beam heating. ***Materials Transactions***, v. 45, p. 850-857, 2004.

Artigo recebido em 13 de março de 2013. Aprovado em 24 de junho de 2013.